*Proc. Natl. Acad. Sci. USA*
Vol. 88, pp. 11535–11539, December 1991
Biochemistry

# How does RNase H recognize a DNA·RNA hybrid?

**(substrate recognition/site-directed mutagenesis/heteronuclear two-dimensional NMR)**

HARUKI NAKAMURA*, YASUSHI ODA*, SHIGENORI IWAI†, HIDEO INOUE†, EIKO OHTSUKA†, SHIGENORI KANAYA*, SHIGENOBU KIMURA*, CHIEKO KATSUDA*, KATSUO KATAYANAGI*, KOSUKE MORIKAWA*, HIROTSUGU MIYASHIRO*, AND MORIO IKEHARA*

*Protein Engineering Research Institute, 6-2-3 Furuedai, Suita, Osaka 565, Japan; and †Faculty of Pharmaceutical Sciences, Hokkaido University, Sapporo 060, Japan

*Communicated by Robert L. Letsinger, August 28, 1991*

ABSTRACT **The mechanism of RNase H substrate recognition is proposed from a model of a chemically modified DNA·RNA hybrid *Escherichia coli* RNase H complex. Site-directed mutagenesis of the enzyme and substrate titration observed by heteronuclear two-dimensional NMR spectra have been carried out. A model complex has been built, based on free structures of the enzyme and the substrate independently determined by x-ray crystallography and NMR distance geometry, respectively. In addition to steric and electrostatic complementarities between the molecular surfaces of the enzyme and the minor groove of the hybrid in the model, putative hydrogen bonds between the polar groups in the enzyme and 2′-oxygens of the RNA strand of the hybrid fix the hybrid close to the active site of the enzyme. The enzymatic activities of the mutant proteins and the changes in NMR spectra during the course of substrate titration are consistent with the present model. Moreover, the specific cleavage of the RNA strand in DNA·RNA hybrids can be explained as well as cleavage modes in modified heteroduplexes. A mechanism of enzymatic action is proposed.**

A unique endoribonuclease named RNase H has the specific function of cleaving the RNA strand of a DNA·RNA hybrid, yielding a 3′-hydroxyl and a 5′-phosphate at the hydrolysis site (1). This enzyme requires $Mg^{2+}$ for its enzymatic activity.

Although the physiological role of RNase H is still unclear, recent studies suggest that the enzyme's function is associated with DNA replication. The importance of this enzyme is also suggested by its existence in organisms from *Escherichia coli* to humans. In addition, the C-terminal domain of retroviral reverse transcriptase is thought to be essentially the same as RNase H (2–4).

RNase H has only a slight specificity for the base sequence of the hybrid. However, Inoue *et al.* (5), using chimeric oligonucleotides containing four successive deoxyribonucleotides among 2′-*O*-methylnucleotides in the DNA strand, observed cleavage of the RNA strand at a specific position. They also found that RNase H does not cleave an oligo-RNA strand in a hybrid with its complementary 2′-*O*-methylnucleotide strand, or a 2′-*O*-methylnucleotide strand hybridized with its complementary DNA strand.

From a series of site-directed mutagenesis experiments (6) and computer analysis of amino acid sequences of RNase H and the C domain of reverse transcriptase from many species (2), the active site residues of *E. coli* RNase H were suggested to be Asp-10, Glu-48, and Asp-70.

Recently, the three-dimensional structure of *E. coli* RNase H has been determined by two independent x-ray crystallographic studies (7, 8). The catalytic action of RNase H seems to be similar to that of DNase I (9), and some similarities have been found in the architecture of the β-sheets around the suggested active site residues Asp-10, Glu-48, and Asp-70. It has also been confirmed by x-ray crystallography (7) that $Mg^{2+}$ binds close to this region.

There are many publications describing the tertiary structures of the DNA·RNA hybrids by NMR (10–12), Raman spectroscopy (13), x-ray fiber diffraction (14, 15), and x-ray crystallography (16). The published results are often incompatible with each other, and it may be considered that hybrids can have A forms, B forms, and heterogeneous forms (DNA strands have B forms and RNA strands have A forms) depending on the solvent conditions and the base sequences. Using two-dimensional NMR techniques and distance geometry calculations, we determined the three-dimensional structure of a hybrid nonanucleotide containing 2′-*O*-methylnucleotides and tetradeoxyribonucleotide and its complementary RNA strand, which is cleaved at a specific position by RNase H. The structure of this hybrid is almost typical A form—that is, the sugar puckerings of the furanose rings of both the strands are all N-type conformations.

In this paper, to clarify the substrate recognition mechanism of *E. coli* RNase H, experiments of site-directed mutagenesis of the enzyme, and substrate titration in the absence of $Mg^{2+}$, observing $^{1}H$–$^{15}N$ heteronuclear two-dimensional NMR spectra, were carried out, and then a model structure of a hybrid complex with RNase H was constructed.

## MATERIALS AND METHODS

**Enzymatic Activities of Site-Directed Mutants.** Plasmid pDR600 was constructed to overproduce *E. coli* RNase H in *E. coli* strain JM109 (6). Site-directed mutagenesis was carried out using the oligonucleotide-directed *in vitro* mutagenesis system (Amersham), and all mutant genes were recloned into plasmid pDR600 as described (6). The activities of the mutant enzymes were determined as described (17), except that a [$^{3}H$]M13 DNA·RNA hybrid was used as a substrate instead of [$^{32}P$]poly(rA)·poly(dT). M13 hybrid was prepared according to the method of Kane (18). Hydrolysis of this substrate by the enzyme was analyzed by the Michaelis–Menten equation. The relative $K_m$ and $k_{cat}$ values of the mutant enzymes compared to the wild-type enzyme vary similarly when using either nonanucleotide hybrid or M13 hybrid as substrate (S. Kanaya, unpublished data).

**Oligonucleotide Titration.** To uniformly label the enzyme by $^{15}N$, *E. coli* strain JM109, in which plasmid pJAL600 (S. Kanaya, unpublished data) was cloned, was grown in the M9 minimum culture medium including $^{15}NH_4Cl$. By increasing the cultivation temperature from 32°C to 42°C, overproduction of the enzyme was induced. After an additional 4-hr cultivation, cells were harvested by centrifugation and sub-

The publication costs of this article were defrayed in part by page charge payment. This article must therefore be hereby marked "*advertisement*" in accordance with 18 U.S.C. §1734 solely to indicate this fact.

Abbreviation: $^{15}N$ SQC, $^{15}N$ single-quantum coherence.

jected to purification procedures with buffers including 1 mM EDTA as described (19). About 15 mg of purified protein can be obtained from 1 liter of culture by this system.

Nonaribonucleotide (GGAGAUGAC) and nonanucleotide containing 2′-*O*-methylnucleotides and tetradeoxyribonucleotide (GmUmCmdAdTdCdTCmCm) were synthesized chemically following the procedure of Inoue *et al.* (5). By mixing these two strands, the nonanucleotide hybrid was prepared.

The enzyme and the hybrid were dissolved in 10 mM acetate buffer (pH 5.5) with 0.3 M KCl and 0.1 mM EDTA of 90% $H_2O$/10% $^2H_2O$. The concentration of the enzyme was 1.1 mM and that of the hybrid was 3.3 mM. In the course of titration, 5–50 μl of hybrid solution was added to the 270-μl enzyme solution. Molar ratios of the nonanucleotide hybrid to the enzyme were 0, 0.05, 0.1, 0.2, 0.3, and 0.5. All the titration measurements were performed at 27°C.

Direct couplings between amide protons and amide $^{15}N$ of the enzyme were observed by using $^1H$-detected $^{15}N$ single-quantum coherence ($^{15}N$ SQC) (20). The pulse sequence proposed by Bax *et al.* (21) was used.

All the NMR spectra were measured with a Bruker AM500 (Silberstreifen, F.R.G.). Proton chemical shifts are relative to the water signal (4.78 ppm). $^{15}N$ chemical shifts are relative to the $^{15}N$ signal of formamide (113.3 ppm).

**Modeling Procedure.** By taking ordinary two-dimensional proton NMR spectra (12) in $^2H_2O$, all nonexchangeable proton chemical shifts of the free nonanucleotide hybrid (GGAGAUGAC/GmUmCmdAdTdCdTCmCm) were determined except all H 5′ and H 5″ and a few H 4′ protons. A series of two-dimensional nuclear Overhauser effect (NOE) spectra were taken with five different mixing times: 25, 50, 75, 100, and 250 ms. From the initial buildup ratios of the NOE signals, the interproton distances between nonexchangeable protons were determined by referring to the standard distance between H-5 and H-6 protons in cytosine.

Table 1. Kinetic constants for *E. coli* RNase H and its mutants

| Mutant | $K_m$, μM | $K_m/K_m$* | $k_{cat}/k_{cat}$† |
|---|---|---|---|
| Wild type | 0.089 | 1 | 1 |
| Cys-13 to Ala | 1.2 | 13.5 | 4.9 |
| Asn-16 to Ala | 3.0 | 33.7 | 3.5 |
| Asn-44 to Ala | 0.67 | 7.5 | 1.0 |
| Asn-45 to Ala | 1.8 | 19.7 | 2.0 |
| Gln-72 to Ala | 0.42 | 4.7 | 1.7 |
| Gln-76 to Ala | 0.18 | 2.0 | 0.9 |
| Gln-80 to Ala | 0.10 | 1.1 | 1.0 |

*$K_m$ in mutant enzymes relative to wild type.
†$k_{cat}$ in mutant enzymes relative to wild type.

Distance geometry calculations using 338 distance restraints reconstructed an almost typical A-form duplex structure. (H.M. and H.N., unpublished data). The structure of this free hybrid and that of the free enzyme with $Mg^{2+}$ determined by x-ray crystallography (7) were displayed simultaneously on the computer graphics screen [Evans and Sutherland (Salt Lake City), PS390], and the initial complex structure was made by manipulating them using the molecular graphics program HYDRA (Polygen, Waltham, MA). Next, fixing both structures, relative distance and orientation were optimized by using an in-house molecular mechanics program, PRESTO (H.N., unpublished data), using the AMBER all-atom force field (22). Finally, while fixing the position of $Mg^{2+}$ and all atoms of the enzyme, except atoms of side chains on the side of the enzyme interacting with the hybrid, the conformation energy of the whole structure was minimized with 338 distance restraints observed for the free hybrid structure using a conjugate gradient method. All the bad contacts were repaired with a small distance violation for the hybrid structure. The nonbonded energy in the final complex structure was −747 kcal/mol (1 cal = 4.184 J) and the total distance violation for 338 distance restraints was 2.5 Å.

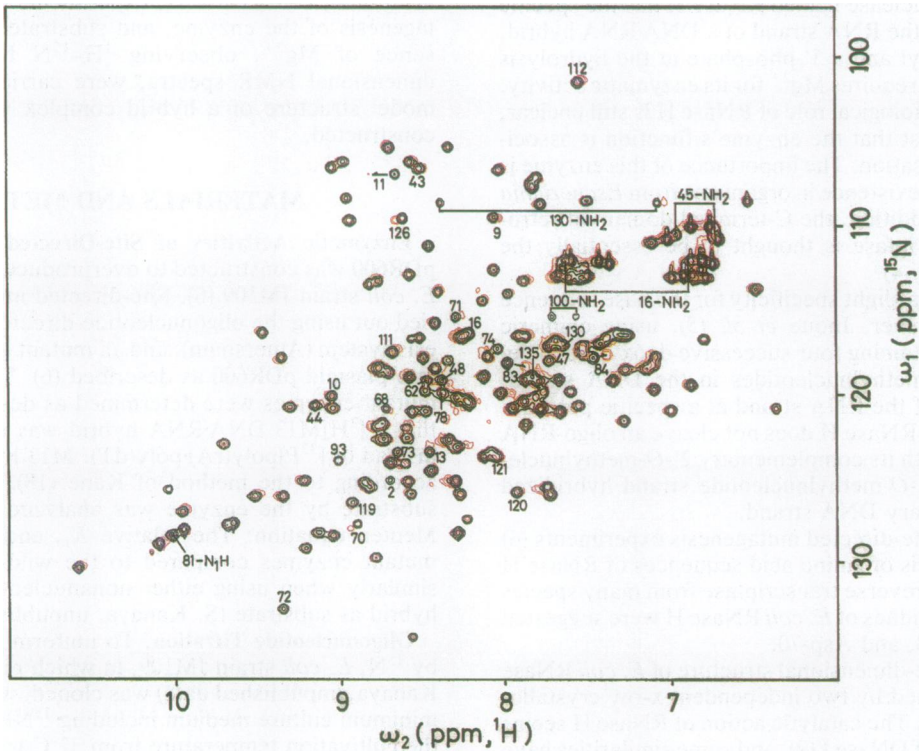


FIG. 1. Backbone amide region in $^1H$-detected $^{15}N$ SQC spectrum of uniformly $^{15}N$-labeled *E. coli* RNase H solution (black). Red indicates the spectrum when mixed with the nonanucleotide hybrid at a molar ratio to the enzyme of 0.3. Numbers indicate residues whose cross peaks changed significantly. Bars and $-NH_2$ indicate the amino groups of asparagine side chains. $N_1H$ indicates the $N_1$-imino group of the tryptophan side chain.

## RESULTS

**Site-Directed Mutagenesis.** Table 1 shows the enzymatic activities of site-directed mutants of *E. coli* RNase H. Evidently, when Cys-13, Asn-16, Asn-44, Asn-45, and Gln-72 are substituted by alanines, the relative $K_m$ of these mutants increases, although the replacements did not much affect the relative $k_{cat}$ values. These replacements are not as lethal as those of residues 10, 48, or 70, whose relative $k_{cat}$ values are $<10^{-3}$ (6), but reduce substrate binding to some extent. Gln-76 and Gln-80 do not seem important for the enzyme's action.

**Oligonucleotide Titration.** In the course of titration with the nonanucleotide hybrid, a large amount of precipitate appeared when the molar ratio of the hybrid to the enzyme exceeded 0.3, and the NMR signal became too weak to observe cross peaks. $^1$H-detected $^{15}$N SQC spectra of uniformly $^{15}$N-labeled *E. coli* RNase H solutions are shown in Fig. 1 for molar ratios 0 and 0.3. The differences in the spectra are not so large as to suggest any large structural changes. During substrate titration, the positions of several cross peaks moved and a few cross peaks became broad, without the appearance of any new cross peaks. This suggests that the complex is not in the slow exchange.

The chemical shift of the backbone protons and $^{15}$N has already been completely assigned to their associated residues in solution at the same pH but without KCl, with the aid of heteronuclear three-dimensional NMR techniques (23) using uniformly $^{15}$N- and $^{13}$C-labeled enzymes and specifically $^{15}$N-labeled enzymes (24). With 0.3 M KCl, most of the cross peaks have chemical shifts similar to those without KCl. Therefore, by observing shifts in the cross peaks in Fig. 1 during substrate titration, the amino acid residues responsible for the hybrid's recognition could be mapped. Since the cross peak of residue 63 could not be observed and the cross peaks of residues 2 and 93 were always observed as weak peaks, their effects could not be considered. Spectra at different molar ratios were successively observed, and the assignment was unambiguous for cross peaks other than those of residues 7, 12, 16, 40, 49, 54, 56, 60, 74, 76, 77, 79, 85, 88, 133, and 138, where peaks overlapped. As shown in Fig. 1, cross peaks between backbone amide $^1$H and $^{15}$N of residues 10, 11, 44, 48, 70, 71, and 73 became broad in the course of titration. Cross peaks associated with the side chains of Asn-16 ($NH_2$), Asn-45 ($NH_2$), and Trp-81 (NH) also broaden. The broadenings of these cross peaks were confirmed from one-dimensional cross section spectra around those peaks. Fig. 2 shows the residues whose chemical shifts changed or broadened significantly, comparing two spectra at the molar ratios 0 and 0.3 shown in Fig. 1.

After the NMR measurements, the solution was tested to determine whether the ribonucleotide strand was cleaved. The HPLC pattern of the heated solution at 60°C indicates that the ribonucleotide chain was cleaved to some extent (maximum, 14%), but most of the ribonucleotide strand remained as the hybrid without being cleaved.

## DISCUSSION

The results of Table 1 and Fig. 2 clearly show the site of interaction of the enzyme with the substrate. Site-directed mutagenesis has already suggested that Asp-10, Glu-48, Asp-70, and $Mg^{2+}$ construct the active site (6). Moreover, since the deoxyribonucleotide strand of the hybrid used here is chemically modified, O-3′ of the 6th uracil nucleotide is specifically stimulated by hydrolysis in the presence of $Mg^{2+}$ and cleaved (5). The phosphate group between the 6th uracil and the 7th guanine nucleotides of the ribonucleotide strand should therefore be close to the active site of the enzyme. Using the above information, it was possible to build an unambiguous model of the complex (Fig. 3), starting from the free structures of the enzyme and the hybrid. A crevice, running from the active site to α-helix II is the only possible site for interaction with the hybrid, as shown in Table 1 and Fig. 2, and as suggested by x-ray studies (7, 8) from steric and electrostatic viewpoints.

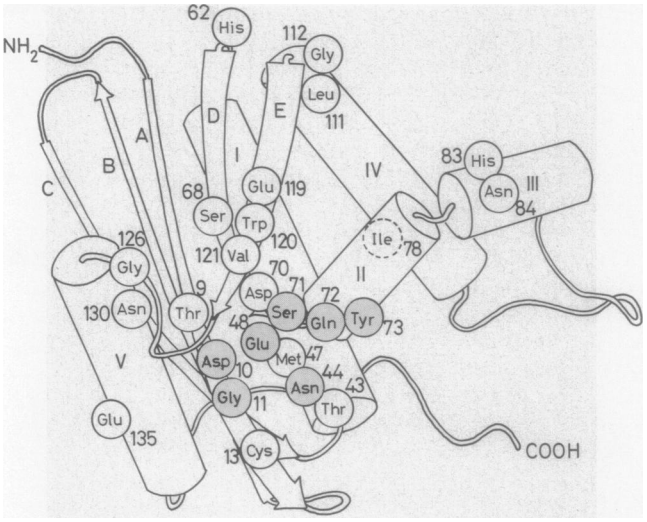


FIG. 2. Positions of residues whose cross peaks have larger absolute chemical shifts than 0.02 ppm in the case of $^1$H or 0.2 ppm in the case of $^{15}$N. Cross peaks of the shaded residues were broadened in the course of titration. The tertiary structure of the enzyme is from Katayanagi *et al.* (7).

Fig. 4 shows the complex model structure around the active site. The specific cleavage site of the ribonucleotide is positioned near the carboxyl groups of Asp-10, Glu-48, and Asp-70 of the enzyme. Strong ionic interactions can be made between these carboxyl groups, $Mg^{2+}$, and the phosphate of the ribonucleotide strand. Besides these electrostatic interactions, there are two putative hydrogen bonds between backbone O-Cys-13 and O-2′ of the 7th guanine, and between N-δ2- or O-δ1-Asn-44 and O-2′ of the 6th uracil. These interactions between O-2′ of the ribonucleotides and the enzyme may play a crucial role in recognition of the ribonu-

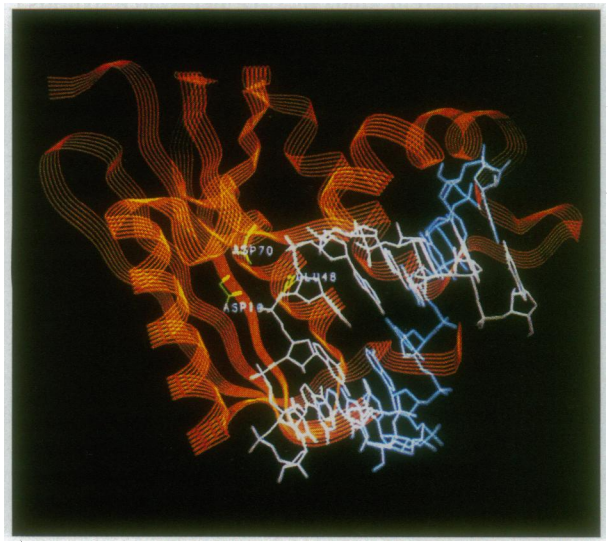


FIG. 3. A DNA·RNA hybrid complex model with *E. coli* RNase H. The ribbon model shows the backbone structure of the enzyme. White wires are the RNA strand and blue wires are the DNA strand. Three carboxylates of Asp-10, Glu-48, and Asp-70 side chains are also shown.

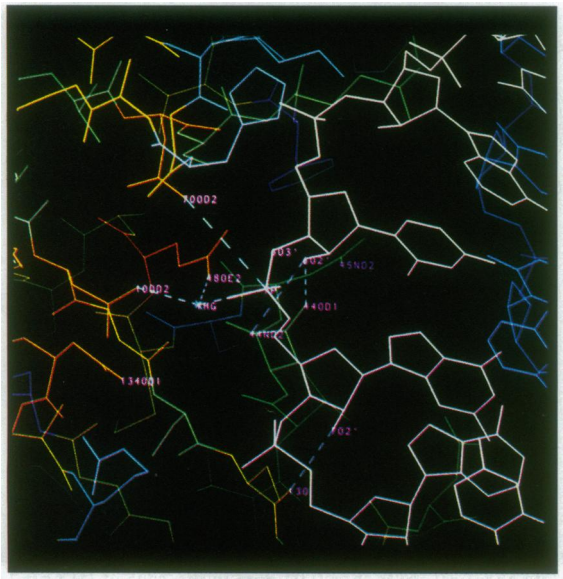

FIG. 4. Complex model structure around the active site. Two putative hydrogen bonds between 2′-hydroxyl groups of RNA strand (white wires) and the enzyme are shown. Dashed lines are between the phosphate of the RNA strand, $Mg^{2+}$, and three carboxylates of Asp-10, Glu-48, and Asp-70.

cleotide chain. The amide group in the side chain of Gln-72 is also close to the bases in the minor groove of the hybrid.

Between the deoxyribonucleotide chain and the enzyme, steric interactions may be dominant. In the model complex, four deoxyribonucleotides interact with the enzyme as shown in Fig. 5. Two 2′-*O*-methylribonucleotides surrounding the four deoxyribonucleotides seem to sterically lock the position of the hybrid to the enzyme. Asn-16 may have an especially important role in this steric interaction. Since the free hybrid has an almost typical A-type structure and the 2′-*O*-methyl groups are far from the cleavage site, chemical modification is not considered to associate directly with specific catalysis of the enzyme. Rather, the locking mechanism is a reasonable interpretation of not only specific cleavage of the current hybrid but also of other cleavage modes in the different kinds of 2′-*O*-methylated hybrids (5).

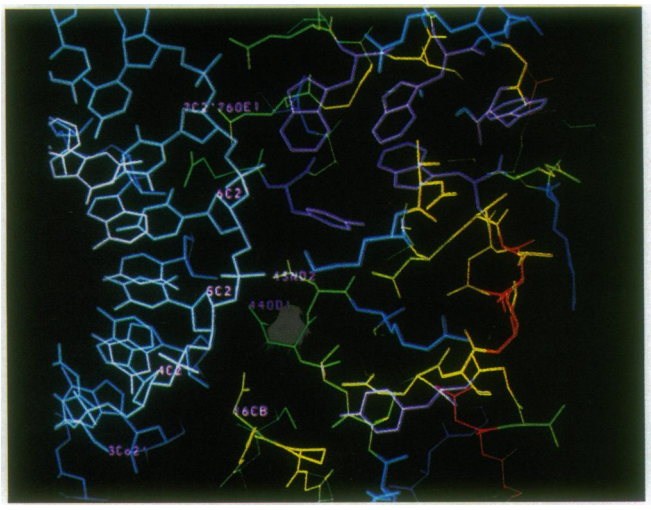

FIG. 5. Interface between the enzyme and the DNA strand in the complex model structure. 4C2′, 5C2′, 6C2′, and 7C2′ indicate 2′-carbons of the DNA strand. These four deoxyribonucleotides are surrounded by 2′-*O*-methylribonucleotides, which seem to lock the hybrid into the enzyme at a specific position.

Current experiments of mutagenesis and titration support this recognition mechanism for the hybrid. It is evident from Table 1 and Fig. 2, that Cys-13, Asn-16, Asn-44, Asn-45, and Gln-72 are engaged in hybrid binding, in addition to the active site residues Asp-10, Glu-48, and Asp-70.

In the titration experiments, changes of the NMR cross peaks associated with His-83, Asn-84, His-62, Leu-111, Gly-112, and Glu-135 were also significant. However, these residues are not close to the substrate recognition site in the present model. For His-83 and Asn-84, the chemical shift change may be due to protonation of the side chain of His-83. Since His-83 is surrounded by positively charged residues, the $pK_a$ is as low as 5.5 in the absence of the substrate (M. Yoshida, personal communication). When negatively charged nucleic acids bind to the enzyme, the $pK_a$ of His-83 should increase. Adding a nucleic acid trimer instead of a nonanucleotide hybrid to the enzyme solution also changed the cross peaks around residue 83 (Y.O. and H.N., unpublished data). His-62, Leu-111, and Gly-112 are positioned in a loop, and local structural change may be induced in the course of titration.

The cleavage modes in modified heteroduplexes (5) are well explained by the present model. When 2′-*O*-hydroxyl groups of the ribonucleotide strand are recognized by the enzyme as proposed, the 2′-*O*-methylnucleotide strand hybridized with its complementary DNA strand cannot be cleaved because of its lack of 2′-*O*-hydroxyls. Moreover, as shown in Fig. 5, recognition of the RNA strand in the hybrid with a complementary 2′-*O*-methylnucleotide strand would be hindered by the 2′-*O*-methyl groups of the other strand, through a steric clash with the enzyme.

In the model shown in Fig. 3, the enzyme interacts with the hybrid's minor groove. It is widely understood that an enzyme that does not recognize a specific base sequence interacts at its minor groove (25). Several studies using chemically modified oligonucleotides (5, 26) also suggest that the enzyme interacts not with the hybrid's major groove but with its minor groove.

A hybrid with the opposite direction to that shown in Fig. 3 could possibly interact with the enzyme. However, in such a model, much fewer interactions were possible than those in the model of Fig. 3, and direct interactions between the hybrid and the residues Cys-13 or Asn-44 could not be found. The chain direction shown in Fig. 3 therefore seems more likely at present.

As described above, DNA·RNA hybrids may generally take many different structures in solution. Arnott *et al.* (15) made a tertiary structure model, in which the RNA chain is a C-3′-endo A-type structure, and DNA is a C-2′-endo B-type structure. Following their coordinates, another hybrid model was constructed with the same base sequence. Notably, the structure of the RNA strand in our model structure is similar to the structure of their RNA strand. This similarity supports the complex model presented here, in which the enzyme mainly recognizes the RNA strand.

When the substrate hybrid is bound to the enzyme, it is possible that the hybrid and the enzyme change their tertiary structures. In fact, it has been observed that in cases of several DNA-binding proteins, such as *Eco*RI endonuclease (27), phage 434 repressor (28), and DNase I (29), backbone structures of the nucleotide duplexes bend when they bind to the enzymes. DNase I is considered to have enzymatic action similar to that of RNase H and x-ray analysis of the DNA duplex complex with DNase I revealed that the DNA duplex kinks in the neighborhood of the binding site (29). In the present complex of the hybrid and the enzyme, both the structures were almost fixed to those of the free forms observed by x-ray and NMR experiments. However, there are several phenomena that suggest some deformation of the hybrid structure in a complex form with the enzyme. For

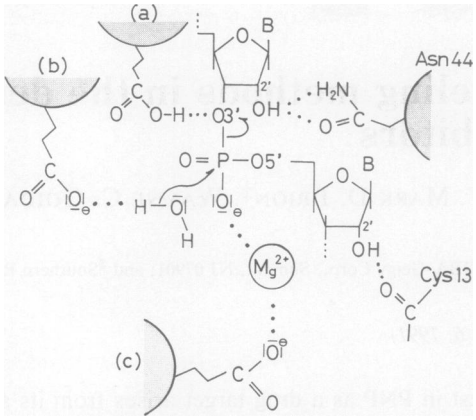


FIG. 6. Schematic drawing of a proposed mechanism for the action of *E. coli* RNase H. Three carboxylates (a, b, and c) are involved in catalytic activity, but they are not definitely identified among Asp-10, Glu-48, and Asp-70. Carboxylate b accepts a proton from a water molecule, which cleaves the P-O-3′ bond. The nucleophile attack of the water molecule is facilitated by electrostatic interactions among a, c, $Mg^{2+}$ ion, and the phosphate. The side chain amide of Asn-44 and the backbone oxygen of Cys-13 make hydrogen bonds with the 2′-hydroxyls of the ribonucleotide chain of the substrate hybrid.

example, a direct interaction between Asn-45 and the hybrid is difficult in the complex model. On the contrary, mutagenesis and titration studies clearly suggest that Asn-45 is involved in substrate binding. As shown in Fig. 4, the side chain of Asn-45 may extend to the most probable position to interact with the bases in the minor groove of the hybrid model. When the hybrid bends between the 5th adenine and the 6th uracil modifying the model, the side chain of Asn-45 can interact directly with the 4th deoxyadenine at the minor groove of the hybrid. This interaction can explain the recent result from chemical modifications of the substrate, where N-3 in the purine ring of the DNA strand is thought to make a hydrogen bond with the enzyme (Y. Miura and E.O., unpublished data). Recently, Wyatt and Walker (26) showed that a ribonucleotide duplex including only two successive deoxyribonucleotides in one strand can be cleaved by *E. coli* RNase H. Since the deoxyribonucleotide chains are considered to be more flexible than the ribonucleotide chains due to hydrated water molecules around 2′-hydroxyls (30), their result may suggest that the hybrid is kinked. Previous experiments introducing pyrophosphate in the hybrid by Metelev *et al.* (31) also support this deformation. Thus, the role of deoxyribonucleotide may be its flexibility to allow the hybrid to kink, so that interaction with the enzyme is enhanced.

From the model structure around the active site shown in Fig. 4, a mechanism of enzymatic action can be suggested, referring to the action of DNase I proposed by Suck and Oefner (9). Since no histidine residues in *E. coli* RNase H are considered to be as crucial as in DNase I, three carboxyl groups are thought to be involved in the enzymatic action as shown in Fig. 6. A water molecule is probably associated with hydrolysis of O-3′ of the ribonucleotide chain. In fact, there is a space between the carboxyl group of Asp-70 and the phosphate, as shown in Fig. 4. It is reasonable that one of the three carboxylates is protonated as a proton donor, because the electrostatic potential in that neighborhood is locally very negative. Since there is no experimental evidence yet to discriminate which carboxyl is protonated, it is difficult to assign a definite role to each carboxyl group. Further experiments are necessary to test this proposal for the mechanism of action.

We thank Mr. T. Yamazaki, Dr. K. Nagayama, and Ms. M. Yoshida for NMR cross peak assignments; Ms. F. Kim for preparation of the enzyme; Dr. T. Ookubo for help in NMR measurements; Dr. Y. Nishimura for discussion; and Dr. T. J. P. Hubbard for reading the manuscript and for discussion.

1. Crouch, R. J. & Dirksen, M.-L. (1982) in *Nuclease*, eds. Linn, S. M. & Roberts, R. J. (Cold Spring Harbor Lab., Cold Spring Harbor, NY), pp. 211–241.
2. Doolittle, R. F., Feng, D.-F., Johnson, M. S. & McClure, M. A. (1989) *Q. Rev. Biol.* **64**, 1–30.
3. Davies, J. F., II, Hostomska, Z., Hostomsky, Z., Jordan, S. R. & Matthews, D. A. (1991) *Science* **252**, 88–95.
4. Nakamura, H., Katayanagi, K., Morikawa, K. & Ikehara, M. (1991) *Nucleic Acids Res.* **19**, 1817–1823.
5. Inoue, H., Hayase, Y., Iwai, S. & Ohtsuka, E. (1987) *FEBS Lett.* **215**, 327–330.
6. Kanaya, S., Kohara, A., Miura, Y., Sekiguchi, A., Iwai, S., Inoue, H., Ohtsuka, E. & Ikehara, M. (1990) *J. Biol. Chem.* **265**, 4615–4621.
7. Katayanagi, K., Miyagawa, M., Matsushima, M., Ishikawa, S., Kanaya, S., Ikehara, M., Matsuzaki, T. & Morikawa, K. (1990) *Nature (London)* **347**, 306–309.
8. Yang, W., Hendrickson, W. A., Crouch, R. J. & Satow, Y. (1991) *Science* **249**, 1398–1405.
9. Suck, D. & Oefner, C. (1986) *Nature (London)* **321**, 620–625.
10. Shindo, H. & Matsumoto, U. (1984) *J. Biol. Chem.* **259**, 8682–8684.
11. Gupta, G., Sarma, M. H. & Sarma, R. H. (1985) *J. Mol. Biol.* **186**, 463–469.
12. Chou, S.-H., Flynn, P. & Reid, B. (1989) *Biochemistry* **28**, 2435–2443.
13. Benevides, J. M. & Thomas, G. J., Jr. (1988) *Biochemistry* **27**, 3868–3873.
14. Zimmerman, S. B. & Pheiffer, B. H. (1981) *Proc. Natl. Acad. Sci. USA* **78**, 78–82.
15. Arnott, S., Chandrasekaran, R., Millane, R. P. & Park, H.-S. (1986) *J. Mol. Biol.* **188**, 631–640.
16. Wang, A. H.-J., Fujii, S., van Boom, J. H., van der Marel, G. A., van Boeckel, S. A. & Rich, A. (1982) *Nature (London)* **299**, 601–604.
17. Kanaya, S. & Crouch, R. J. (1983) *J. Biol. Chem.* **258**, 3187–3196.
18. Kane, C. M. (1988) *Biochemistry* **27**, 3187–3196.
19. Kanaya, S., Kohara, A., Miyagawa, M., Matsuzaki, T., Morikawa, K. & Ikehara, M. (1989) *J. Biol. Chem.* **264**, 11546–11549.
20. Bodenhousen, G. & Ruben, D. G. (1980) *Chem. Phys. Lett.* **69**, 185–189.
21. Bax, A., Ikura, M., Kay, L. E., Torchia, D. A. & Tschudin, R. (1990) *J. Magn. Reson.* **86**, 304–318.
22. Weiner, S. J., Kollman, P. A., Nguyen, D. T. & Case, D. A. (1986) *J. Comput. Chem.* **7**, 230–252.
23. Nagayama, K., Yamazaki, T., Yoshida, M., Kanaya, S. & Nakamura, H. (1990) *J. Biochem. (Tokyo)* **108**, 149–152.
24. Yamazaki, T., Yoshida, M., Kanaya, S., Nakamura, H. & Nagayama, K. (1991) *Biochemistry* **30**, 6036–6047.
25. Seeman, N. C., Rosenberg, J. M. & Rich, A. (1976) *Proc. Natl. Acad. Sci. USA* **73**, 804–808.
26. Wyatt, J. R. & Walker, G. T. (1989) *Nucleic Acids Res.* **17**, 7833–7842.
27. McClarin, J. A., Frederick, C. A., Wang, B.-C., Greene, P., Boyer, H. W., Grable, J. & Rosenberg, J. M. (1986) *Science* **234**, 1526–1541.
28. Anderson, J. E., Ptashne, M. & Harrison, S. C. (1987) *Nature (London)* **326**, 846–852.
29. Suck, D., Lahm, A. & Oefner, C. (1988) *Nature (London)* **332**, 464–468.
30. Saenger, W. (1984) in *Principles of Nucleic Acid Structure* (Springer, New York), Chap. 17.4.
31. Metelev, V. G., Zayakina, G. V., Ryabushenko, I. L., Krynetskaya, N. F., Romanova, E. A., Oretskaya, T. S. & Shabarova, Z. A. (1988) *FEBS Lett.* **226**, 232–234.